Optica Applicata, Vol. XLIII, No. 4, 2013
DOI: 10.5277/oa130418

Slow light effect with low group velocity and low dispersion by adjusting parameters of elliptical scatterers for terahertz frequency

YONG WAN*, YUE GUO, YONGCHENG ZHANG, MAOJIN YUN

College of Physics Science, Qingdao University, Qingdao, 266071, China

*Corresponding author: wanyongqd@hotmail.com

Elliptical scatterers possess the properties of anisotropy and multiple degrees of freedom. With the plane wave expansion method, the slow light effect with high n_g and low dispersion can be achieved by optimizing the structure parameters of photonic crystal waveguide with line defect, including changing the length of major axis or minor axis, and rotating scatterers relative to the direction of line defect. With operating frequency f = 1 THz (wavelength λ = 300 μm), the simulation shows: 1) selecting the group index n_g from 38.5 to 107.4, slow light with low-dispersion bandwidth (n_g varies within a 10% range) from 0.385 to 1.272 μm, ultralow--dispersion bandwidth (n_g varies within a 1% range) from 0.188 to 0.548 μm, and scalar product $n_g\Delta\lambda/\lambda$ from 0.138 to 0.180 were obtained by changing the length of major axis or minor axis; 2) selecting the group index n_g from 38.6 to 107.7, slow light with low-dispersion bandwidth from 0.436 to 1.443 μm, ultralow-dispersion bandwidth from 0.201 to 0.907 μm, and scalar product $n_g\Delta\lambda/\lambda$ from 0.157 to 0.186 were achieved by rotating scatterers θ = 30° relative to the direction of line defect. Moreover, slow light with near-zero dispersion (dispersion parameter D less than 0.01 ps/mm·nm) can also be obtained by these methods, which implies that choosing suitable scatterers and adjusting their parameters we can efficiently achieve slow light with high n_g with wideband and low dispersion.

Keywords: elliptical, scatterer, slow light, dispersion, photonic crystal, waveguide.

1. Introduction

Slow light has relatively low group velocity, and it is widely used for compact optical delay lines, optical buffers and other applications. Slow light in photonic crystals has an incomparable advantage in microphotonic sensors, integrated laser amplifiers, and devices, for its small and compact structure, high transmission efficiency, proper behavior at room temperature and other advantages [1–5]. There are mainly two types of photonic crystal waveguides (PCW) for slow light, namely the line defect waveguide and the coupled resonator waveguide. Unfortunately, large dispersion occurs in both when low group velocity is attempted. So far researchers have discovered that the line

defect waveguide normally results in large group velocity but small dispersion, while the coupled resonator waveguide normally leads to small group velocity but large dispersion [6, 7]. Therefore, many researchers like to use the line defect waveguide to obtain proper slow light with low dispersion.

Several successful attempts with the line defect waveguide were made to effectively obtain slow light with wideband and low dispersion; these methods include adjusting the width of line defect [8, 9], changing the PCW parameters by shifting anticrossing points [10], using slotted photonic crystal waveguides [11, 12], adjusting the diameters of the holes [13, 14], introducing a hetero group velocity waveguide [15, 16], shifting the first and second rows of air holes or shifting the lattice along the waveguide defects [17, 18], infiltrating microfluid into the air holes [19, 20] or using a technique based on selective liquid infiltrations to precisely and reversibly change the structures [21], *etc*. However, the above-mentioned researches focused on the periodic arrangement of the structure, and most of the scatterers are cylindrical, while only in few researches the shape of scatterers was altered [22, 23].

In this paper, elliptical scatterers, which have multiple degrees of freedom for greater manipulation, were applied to photonic crystal line defect waveguide, and by adjusting the parameters including the lengths of major and minor axis, and the angle between the major axis and the line defect, high n_g and thus low group velocity are achieved under low (n_g varies within a 10% range), ultralow (n_g varies within a 1% range), and near zero dispersion (dispersion parameter D less than 0.01 ps/mm·nm), respectively. Thus the performance of slow light waveguide was much improved.

2. Simulation

Figure 1 is a demonstration of line defect waveguides consisting of elliptical scatterers: in Fig. 1**a** the major axis is parallel with the direction of the line defect, and in Fig. 1**b** the angle between the major axis and the line defect is θ. For the ease of analysis, both waveguides have a triangular lattice structure, and the line defect is assigned to the centre line of the structure. We assume that the material is silicon ($n_{Si} = 3.5$) and the working frequency is 1 THz (wavelength $\lambda = 300$ μm), then we define the lattice constant of the structure as a, the radius of the major axis of

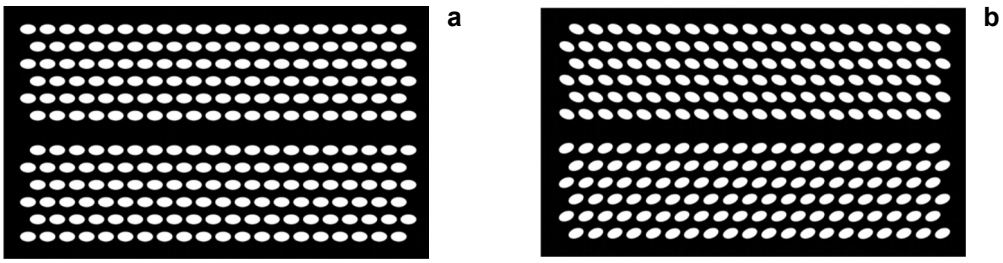

Fig. 1. The schematic diagram of line defect waveguide with elliptical scatterers: major axis is parallel to the direction of line defect (**a**); major axis is θ angle with the direction of line defect (**b**).

the elliptical scatterers as b and that of the minor axis as c, and finally we define a new parameter e as $e = 1 - c/b$, with the range from 0 to 1.

The simulation process for the structure is shown in Fig. 1**a**. We should adjust the parameters b and e (and thus c) according to the lattice constant a to find the appropriate bandgap and the acceptably wide and flat band region for a transverse electric-like (TE) polarized mode with each given n_g, then we finely adjust the parameter b and e while keeping the parameter θ constant. To find a wide and smooth slow light mode for Fig. 1**b** structure, we should also change the parameter θ and finely adjust the parameter b to find an appropriately slow light mode. In the supercell calculation, based on the plane wave expansion (PWE) method, we selected the number of plane waves in each axis as 32 and the eigenvalue tolerance as 10^{-8} for sufficient calculation precision.

The established relationship between n_g and dispersion could be represented by the following formula [24]:

$$n_g = \frac{a}{2\pi}\frac{\mathrm{d}k}{\mathrm{d}f} \tag{1}$$

For slow light, normally $n_g \gg n_{\mathrm{eff}}$, n_{eff} is the effective group refractive index, and the normalized frequency could be expressed as $f = \omega a/2\pi c$, ω is the central angle frequency of the incident pulse, the relationship between the two is $k = 2\pi n_{\mathrm{eff}}/\lambda$, while λ is the wavelength corresponding to the working frequency. To obtain low dispersion, n_g must be kept constant, which means that within a certain range of frequency, f and k have a linear relationship.

2.1. Simulation when the major axis is parallel with the direction of line defect

For the waveguide with the major axis and line defect in parallel, large n_g and flat wideband could be achieved by adjusting the parameters a, b and e. Figure 2**a** shows the variation of f and k as the parameters b and e vary in TE mode. The linear region of each curve represents the ideal slow light region, and the gradient is the value of n_g. It is observed that around $b = 0.400a$, linear region is not well achieved for cylindrical air holes ($e = 0$), while it is well achieved for elliptical scatterers with e from 0.37 to 0.45.

Figure 2**b** corresponds to the structure in Fig. 1**a** and it shows the relationship between n_g and f. Elliptical scatterers lead to proper linear regions (low dispersion region of slow light) on the n_g curves when $n_g = 38.5$, 54.4, 79.8, and 107.4, respectively.

The relationship between n_g and working frequency represented in Fig. 2**b** does not vary if the structure scales proportionately. Therefore, if the working frequency changes, low dispersion structure could be maintained by scaling the structure according to the formula $a = f\lambda$. For instance, when $\lambda = 300$ μm, the value of a should be around 64.8 μm; when $\lambda = 30$ μm, the value of a should be around 6.48 μm, *etc*. On the other hand, in order to obtain near-zero dispersion, the parameter a should be

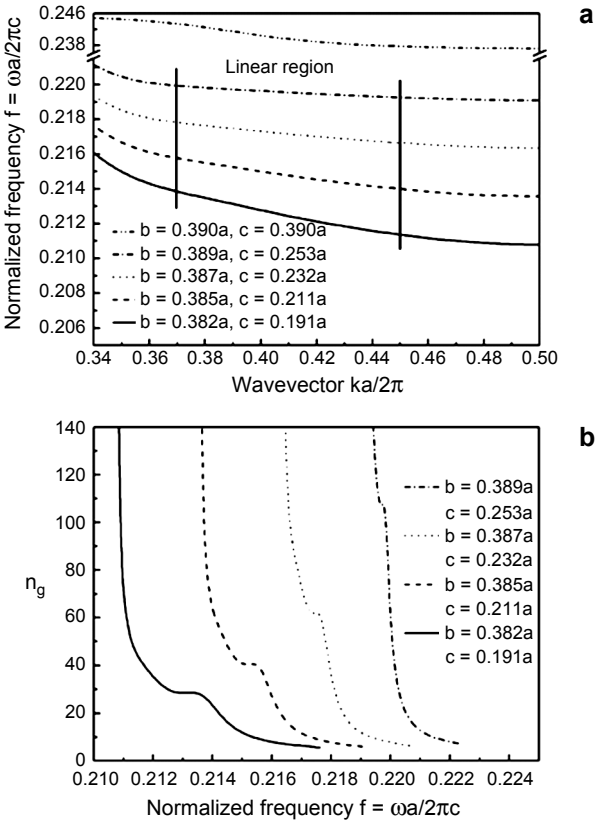

Fig. 2. The relationship between f and k (**a**) and the relationship between n_g and f (**b**) for the structure in Fig. 1**a**.

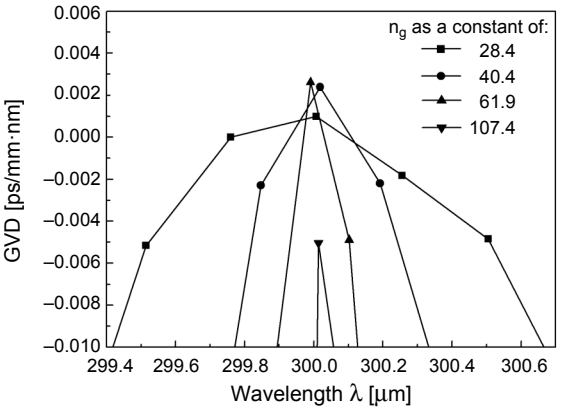

Fig. 3. Dispersion parameter D as a function of wavelength for the Fig. 1**a** structure under different n_g.

finely adjusted according to the bandgap curve. A few groups of corresponding values are $n_{g1} = 38.5$, $a_1 = 64.49$ μm; $n_{g2} = 54.4$, $a_2 = 65.07$ μm; $n_{g3} = 79.8$, $a_3 = 65.57$ μm; $n_{g4} = 107.4$, $a_4 = 65.92$ μm.

To analyze the relationship between low dispersion and wideband in Fig. 2**b**, we define the variable D to describe the relationship between dispersion and wavelength as the following formula [21]:

$$D = \frac{1}{c}\frac{\partial n_g}{\partial \lambda} \tag{2}$$

According to formula (2), if the gradient of $n_g(\lambda)$ approaches zero, D will be near zero, so will be the dispersion. Figure 3 shows the variation of D around working wavelength of 300 μm with different values of n_g. It is observed that D is small, almost zero, when the wavelength is approximately the working wavelength. Besides, the curve is smoother when n_g is smaller.

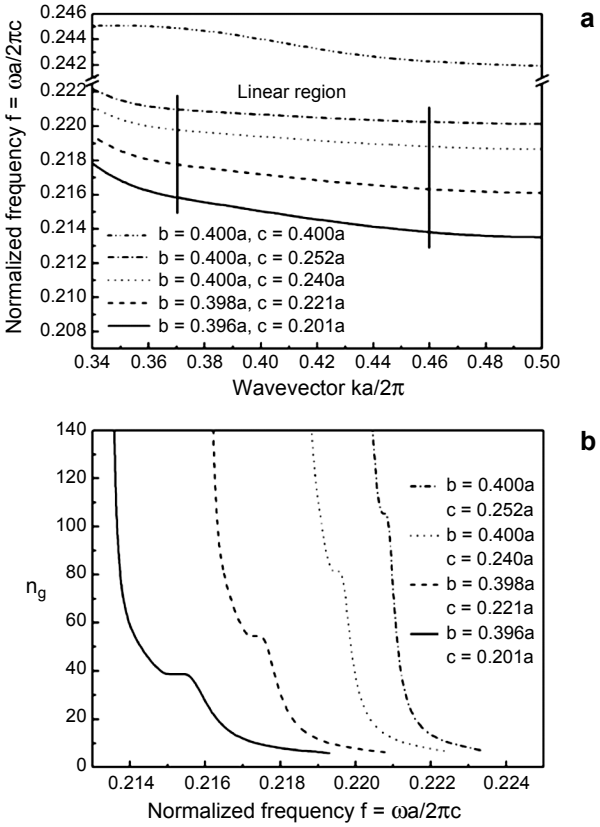

Fig. 4. Relationship between f and k (**a**) and relationship between n_g and f (**b**) for the structure when $\theta = 30°$ in Fig. 1**b**.

2.2. Simulation when the major axis has θ angle with line defect

Since elliptical scatterers are axial symmetrical, large n_g, slow light with wideband and low dispersion could be achieved by rotating the scatterers by θ relative to the line defect and finely adjusting the parameters b and e. Figure 4**a** shows the variation of f and k as the parameters b and e change in TE mode when $\theta = 30°$. It is observed that when b is approximately $0.440a$, elliptical scatterers lead to a proper linear region between 0.37 and 0.46. Figure 4**b** corresponds to the relationship between n_g and f in Fig. 1**b**, and the values n_g of elliptical scatterers are selected as 38.6, 54.6, 81.4, and 107.7, respectively. For the same n_g, the bandwidth of low-dispersion slow light is wider in Fig. 4**b** than in Fig. 2**b**.

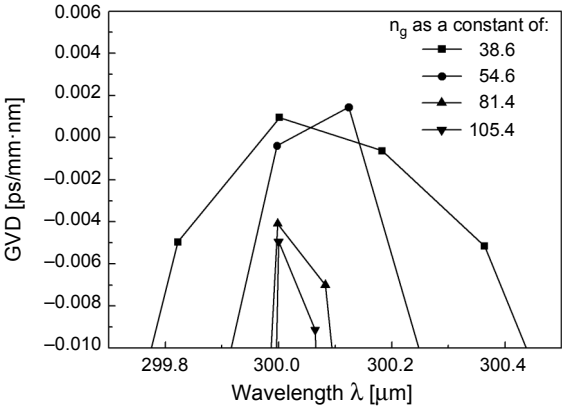

Fig. 5. Dispersion parameter D as a function of wavelength for the Fig. 1**b** structure when $\theta = 30°$ (n_g is 38.6, 54.4, 79.8 and 107.4, respectively).

After $\theta = 30°$ rotation of the major axis with respect to line defect, the bandwidth is larger than that without rotation, when D has the same value and n_g is only slightly different, as shown in Fig. 5. In other words, the value of n_g will be higher than that in Fig. 3, with the same value D and bandwidth.

3. Results and discussion

3.1. Analysis of the result when the major axis is parallel with line defect

To evaluate low dispersion slow light, most previous researches define a range of ±10% of n_g as low dispersion. To further categorize low dispersion, our paper defines a range of ±1% of n_g as ultra-low dispersion, and a range of 0.01 ps/mm·nm of D (less than ±0.5% of n_g) as near-zero dispersion.

Better slow light is achieved when elliptical scatterers substitute cylindrical air holes and the major axis is parallel to the line defect. To illustrate this, the information in Fig. 2**b** is transferred to Table 1. In Table 1, the largest value of n_g is 107.4,

T a b l e 1. Group index and bandwidth under different parameters for structure from Fig. 1**a**.

b	c	n_g	$\Delta\lambda$ ±10% [μm]	$\Delta\lambda$ ±1% [μm]	$n_g\Delta\lambda/\lambda$
0.210a	0.384a	38.5	1.272	0.548	0.163
0.227a	0.387a	54.4	0.993	0.378	0.180
0.242a	0.389a	79.8	0.596	0.323	0.159
0.253a	0.389a	107.4	0.385	0.188	0.138

the largest wideband within ±1% variation is 0.548 μm, and the largest wideband within ±10% variation is 1.272 μm, and scalar product $n_g\Delta\lambda/\lambda$, which stands for group index times normalized bandwidth, is from 0.138 to 0.180. These sets of data are quite useful due to their high refractive index and ultra-low dispersion wideband.

The explanation of this phenomenon is as follows: slow light dispersion of photonic crystal waveguide consists of mainly backscattering and omnidirectional reflection. For cylindrical scatterers, backscattering is more significant, thus the methods like reducing width of line defect, adopting slit photonic crystal waveguides, adjusting the radius of air holes or substituting scatterers with elliptical ones are applied to enhance the performance. However, if different types of scatters are used in the same structure, omnidirectional reflection would be increased and thus slow light is undermined. Fortunately, if elliptical scatterers are adopted, backscattering could be controlled by varying the parameters b and e, and omnidirectional reflection could be contained since only one type of scatterers is adopted, therefore dispersion is largely reduced. This explains the large wideband (ultra-low dispersion region) and large n_g achieved by applying elliptical scatterers, as shown in Fig. 2.

As mentioned earlier, to achieve near-zero dispersion, sometimes the parameter a needs to be finely adjusted. For instance, when working wavelength λ is 300 μm, a_1 is set at 64.49 μm if $n_{g1} = 38.5$, and a_2 is set at 65.07 μm if $n_{g2} = 54.4$, in order to achieve near-zero dispersion.

To analyze the near-zero dispersion region, the information about the parameter D in Fig. 4 is transferred into Table 2. From Table 2, it is observed that slow light bandwidth exceeds 0.39 μm when $n_g = 38.5$ and D varies within ±0.005 ps/mm·nm; slow light bandwidth exceeds 0.05 μm when $n_g = 107.4$ and D varies within ±0.01 ps/mm·nm. The distortion of internal transmission of light pulses is negligible, since these structures have very small values of D.

T a b l e 2. Dispersion parameter D under $\Delta\lambda$ for different group index in structure from Fig. 1**a**.

n_g	a [μm]	$\lvert D\rvert$ [ps/mm·nm]	$\Delta\lambda$ [μm]
38.5	64.49	≤ 0.005	0.39
54.4	65.07	≤ 0.005	0.19
79.8	65.57	≤ 0.010	0.10
107.4	65.92	≤ 0.010	0.05

3.2. Analysis of the result when the major axis has θ angle with line defect

There are two approaches to rotate elliptical scatterers by θ angle with respect to line defect: rotate all scatterers in the same direction and rotate the scatterers axial symmetrically about the line defect. After refining the parameters, both approaches lead to similar values of n_g, but the latter performs much better in terms of the flat region in slow light curve and is therefore adopted in this paper.

As the value of θ changes, slow light effect varies, and the condition to achieve ideal slow light effect changes too. Simulation has shown that proper slow light is obtained when the value of θ is in the range of 0 to 60° (we just give $\theta = 30°$ as an example here). If θ changes and so do the bandgap and the slow light mode, the group index and the flat bandwidth better than those when major axis is parallel with line defect could be achieved by adjusting the parameter b.

Table 3 is established from the information in Fig. 4**b**. For the quite nearly value of n_g, the bandwidths of the flat region for low and ultra-low dispersion (range of variation of n_g is within ±10% and ±1%, respectively) become larger than those in Tab. 1. In comparison, $n_g = 38.5$ corresponds to 1.272 μm and 0.548 μm in Tab. 1, $n_g = 38.6$ corresponds to 1.443 μm and 0.907 μm in Tab. 3; $n_g = 54.4$ corresponds to 0.993 μm and 0.378 μm in Tab. 1, $n_g = 54.6$ corresponds to 1.004 μm and 0.504 μm in Tab. 3; $n_g = 107.4$ corresponds to 0.385 μm and 0.188 μm in Tab. 1, $n_g = 107.7$ corresponds to 0.436 μm and 0.201 μm in Tab. 3. The scalar product $n_g \Delta\lambda/\lambda$ is from 0.157 to 0.186, which is also better than that in Tab. 1.

For further comparison of the near-zero dispersion region, sets of data in Fig. 5 are transferred into Tab. 4. It is observed that the near-zero bandwidth is larger than that without rotation in Table 2. For example, slow light bandwidth exceeds 0.55 μm when

T a b l e 3. Group index and bandwidth under different parameters for the Fig. 1**b** structure when $\theta = 30°$.

b	c	n_g	$\Delta\lambda$ ± 10% [μm]	$\Delta\lambda$ ± 1% [μm]	$n_g\Delta\lambda/\lambda$
0.201a	0.396a	38.6	1.443	0.907	0.186
0.221a	0.398a	54.6	1.004	0.504	0.183
0.240a	0.400a	81.4	0.662	0.342	0.180
0.253a	0.400a	107.7	0.436	0.201	0.157

T a b l e 4. Dispersion parameter D under $\Delta\lambda$ for different group index in structure from Fig. 1**a** and for the Fig. 1**b** structure when $\theta = 30°$.

n_g	a [μm]	$\lvert D\rvert$ [ps/mm·nm]	$\Delta\lambda$ [μm]
38.6	64.59	≤ 0.005	0.55
54.6	65.21	≤ 0.005	0.24
81.4	65.86	≤ 0.010	0.14
107.7	66.26	≤ 0.010	0.08

n_g = 38.6 and D varies within ±0.005 ps/mm·nm; slow light bandwidth exceeds 0.08 μm when n_g = 107.7 and D varies within ±0.01 ps/mm·nm.

3.3. Clarifications

Though our research consists of theoretical analysis and simulation, instead of practical fabrication, we would like to mention the acceptable tolerance of fabrication. The fabrication error was simulated with additional simulations with values around the exact value, and so far the acceptable tolerance of fabrication is ±20 nm. This is the reason that we choose f = 1 THz (wavelength λ = 300 μm) as operating frequency. Taking n_g = 38.5 as an example, a = 64.49 μm, according to the optimized parameters listed in Table 1, we tuned the parameters b slightly, and the results are shown in Fig. 5. In Fig. 6, we chose four values (+40 nm, +20 nm, –20 nm and –40 nm) around the exact value of b (b = 0.253a = 16.32 μm) and ran additional simulations with these four values. The solid curve corresponds to the ideal model without any fabrication error. We can see from Fig. 6 that the flat band part of the curve remains almost unchanged around n_g = 38.5 when the fabrication error is within ±40 nm. The simulation result is the same when the fabrication error is within ±40 nm even for operating frequency f = 0.1 THz, and this precision can be achieved with e-beam lithography very well now.

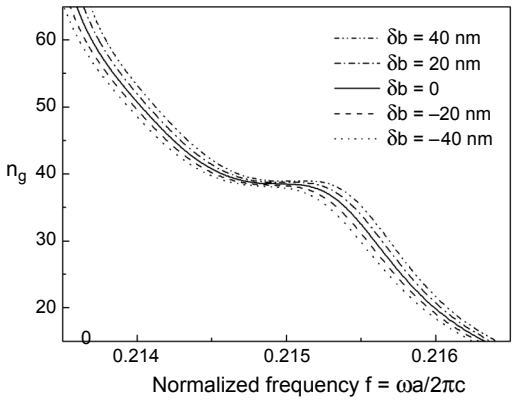

Fig. 6. Parameter n_g as a function of normalized frequency with fabrication errors relative to parameter b when n_g = 38.5 as listed in Table 1.

But for operating wavelength 1550 nm (a = 335.0 nm), the fabrication error must be within ±1 nm, and this precision cannot be achieved with e-beam lithography. So the current fabrication error could reach ±20 nm, less sufficient than the requirement of our research, therefore the structure in our research could be applied to THz and other electromagnetic waves with relatively larger wavelength. In addition, it is ex-

pected that the fabrication error would continue to decrease with advancement of technology, and thus the scope of application of our research will broaden.

4. Conclusions

By applying photonic crystal line defect with elliptical scatterers, adjusting the lengths of the major axis and that of the minor axis, and changing the angle of rotation of the scatterers one can effectively reduce the influence of backscattering and omnidirectional reflection, achieve low dispersion, high group refractive index and low group velocity, and greatly enhance the performance of slow light waveguide. The significance of our research is that slow light with low dispersion and flat wideband could be achieved by adopting new types of scatterers and adjusting their parameters, just like changing periodic arrays.

Acknowledgments – This work is supported by the National Natural Science Foundation of China (NSFC, 11144007), and the Science Foundation of Shandong Province (No. BS2012CL012).

References

[1] ZHIMIN SHI, BOYD R.W., GAUTHIER D.J., DUDLEY C.C., *Enhancing the spectral sensitivity of interferometers using slow-light media*, Optics Letters **32**(8), 2007, pp. 915–917.

[2] BABA T., *Slow light in photonic crystals*, Nature Photonics **2**(8), 2008, pp. 465–473.

[3] KRAUSS T.F., *Slow light in photonic crystal waveguides*, Journal of Physics D: Applied Physics **40**(9), 2007, pp. 2666–2670.

[4] ASSEFA S., MCNAB S.J., VLASOV Y.A., *Transmission of slow light through photonic crystal waveguide bends*, Optics Letters **31**(6), 2006, pp. 745–747.

[5] CHUNFANG OUYANG, DEZHUAN HAN, FANGYUAN ZHAO, XINHUA HU, XIAOHAN LIU, JIAN ZI, *Wideband trapping of light by edge states in honeycomb photonic crystals*, Journal of Physics: Condensed Matter **24**(49), 2012, article 492203.

[6] ENGELEN R.J.P., SUGIMOTO Y., WATANABE Y., KORTERIK J.P., IKEDA N., VAN HULST N.F., ASAKAWA K., KUIPERS L., *The effect of higher-order dispersion on slow light propagation in photonic crystal waveguides*, Optics Express **14**(4), 2006, pp. 1658–1672.

[7] PETROV A.YU., EICH M., *Zero dispersion at small group velocities in photonic crystal waveguides*, Applied Physics Letters **85**(21), 2004, pp. 4866–4868.

[8] DI FALCO A., O'FAOLAIN L., KRAUSS T.F., *Dispersion control and slow light in slotted photonic crystal waveguides*, Applied Physics Letters **92**(8), 2008, article 083501.

[9] CHUNFANG OUYANG, ZHIQIANG XIONG, FANGYUAN ZHAO, BIQIN DONG, XINHUA HU, XIAOHAN LIU, JIAN ZI, *Slow light with low group-velocity dispersion at the edge of photonic graphene*, Physical Review A **84**(1), 2011, article 015801.

[10] BOWEN WANG, DÜNDAR M.A., NÖTZEL R., KAROUTA F., SAILING HE, VAN DER HEIJDEN R.W., *Photonic crystal slot nanobeam slow light waveguides for refractive index sensing*, Applied Physics Letters **97**(15), 2010, article 151105.

[11] KUBO S., MORI D., BABA T., *Low-group-velocity and low-dispersion slow light in photonic crystal waveguides*, Optics Letters **32**(20), 2007, pp. 2981–2983.

[12] FRANDSEN L.H., LAVRINENKO A.V., FAGE-PEDERSEN J., BOREL P.I., *Photonic crystal waveguides with semi-slow light and tailored dispersion properties*, Optics Express **14**(20), 2006, pp. 9444–9450.

[13] O'FAOLAIN L., YUAN X., MCINTYRE D., THOMS S., CHONG H., DE LA RUE R.M., KRAUSS T.F., *Low--loss propagation in photonic crystal waveguides*, Electronics Letters **42**(25), 2006, pp. 1454–1455.

[14] CHANGHONG LI, HUIPING TIAN, CUI ZHENG, YUEFENG JI, *Improved line defect structures for slow light transmission in photonic crystal waveguide*, Optics Communications **279**(), 2007, pp. 214–218.

[15] OZAKI N., KITAGAWA Y., TAKATA Y., IKEDA N., WATANABE Y., MIZUTANI A., SUGIMOTO Y., ASAKAWA K., *High transmission recovery of slow light in a photonic crystal waveguide using a hetero groupvelocity waveguide*, Optics Express **15**(13), 2007, pp. 7974–7483.

[16] WHITE T.P., BOTTEN L.C., MARTIJN DE STERKE C., DOSSOU K.B., MCPHEDRAN R.C., *Efficient slow--light coupling in a photonic crystal waveguide without transition region*, Optics Letters **33**(22), 2008, pp. 2644–2646.

[17] JUNTAO LI, WHITE T.P., O'FAOLAIN L., GOMEZ-IGLESIAS A., KRAUSS T.F., *Systematic design of flat band slow light in photonic crystal waveguides*, Optics Express **16**(9), 2008, pp. 6227–6232.

[18] FENG-CHUN LENG, WEN-YAO LIANG, BIN LIU, TONG-BIAO WANG, HE-ZHOU WANG, *Wideband slow light and dispersion control in oblique lattice photonic crystal waveguides*, Optics Express **18**(6), 2010, pp. 5707–5712.

[19] JUN WU, YANPING LI, CHAO PENG, ZIYU WANG, *Wideband and low dispersion slow light in slotted photonic crystal waveguide*, Optics Communications **283**(14), 2010, pp. 2815–2819.

[20] EBNALI-HEIDARI M., GRILLET C., MONAT C., EGGLETON B.J., *Dispersion engineering of slow light photonic crystal waveguides using microfluidic infiltration*, Optics Express **17**(3), 2009, pp. 1628–1635.

[21] HAMACHI Y., KUBO S., BABA T., *Slow light with low dispersion and nonlinear enhancement in a lattice-shifted photonic crystal waveguide*, Optics Letters **34**(7), 2009, pp. 1072–1074.

[22] JUN WU, YANPING LI, CHAO PENG, ZIYU WANG, *Numerical demonstration of slow light tuning in slotted photonic crystal waveguide using microfluidic infiltration*, Optics Communications **284**(8), 2011, pp. 2149–2152.

[23] SETTLE M.D., ENGELEN R.J.P., SALIB M., MICHAELI A., KUIPERS L., KRAUSS T.F., *Flatband slow light in photonic crystals featuring spatial pulse compression and terahertz bandwidth*, Optics Express **15**(1), 2007, pp. 219–226.

[24] YONG WAN, KAI FU, CHANGHONG LI, MAOJIN YUN, *Improving slow light effect in photonic crystal line defect waveguide by using eye-shaped scatterers*, Optics Communications **286**(1), 2013, pp. 192–196.

Received January 9, 2013
in revised form March 27, 2013